A semi-analytical solver for the Grad-Shafranov equation

D. Ciro and I. L. Caldas

Articles you may be interested in

A similarity reduction of the Grad–Shafranov equation
Phys. Plasmas **17**, 074502 (2010); 10.1063/1.3456519

Symmetry analysis of the Grad–Shafranov equation
Phys. Plasmas **16**, 123101 (2009); 10.1063/1.3267211

Analytic, high-β solutions of the helical Grad–Shafranov equation
Phys. Plasmas **11**, 3752 (2004); 10.1063/1.1763576

Analytical solutions to the Grad–Shafranov equation
Phys. Plasmas **11**, 3510 (2004); 10.1063/1.1756167

Analytical solutions to the Grad–Shafranov equation for tokamak equilibrium with dissimilar source functions
Phys. Plasmas **6**, 3554 (1999); 10.1063/1.873630

A semi-analytical solver for the Grad-Shafranov equation

D. Ciro[a)] and I. L. Caldas[b)]
Departamento de Física Aplicada, Universidade de São Paulo, 05508-090, São Paulo, Brazil

In toroidally confined plasmas, the Grad-Shafranov equation, in general, a non-linear partial differential equation, describes the hydromagnetic equilibrium of the system. This equation becomes linear when the kinetic pressure is proportional to the poloidal magnetic flux and the squared poloidal current is a quadratic function of it. In this work, the eigenvalue of the associated homogeneous equation is related with the safety factor on the magnetic axis, the plasma beta, and the Shafranov shift; then, the adjustable parameters of the particular solution are bounded through physical constrains. The poloidal magnetic flux becomes a linear superposition of independent solutions and its parameters are adjusted with a non-linear fitting algorithm. This method is used to find hydromagnetic equilibria with normal and reversed magnetic shear and defined values of the elongation, triangularity, aspect-ratio, and X-point(s). The resultant toroidal and poloidal beta, the safety factor at the 95% flux surface, and the plasma current are in agreement with usual experimental values for high beta discharges and the model can be used locally to describe reversed magnetic shear equilibria. © 2014 AIP Publishing LLC. [http://dx.doi.org/10.1063/1.4901036]

I. INTRODUCTION

The solution of the Grad-Shafranov equation[1–3] provides the magnetic field, the current density, and the kinetic pressure inside an axisymmetric plasma in hydromagnetic equilibrium. Having analytical solutions to this equation is convenient to configure physical equilibria as a basis for theoretical studies of transport, waves, and stability. It also allows to estimate the external magnetic field configuration necessary to confine a toroidal plasma with specified parameters.[4]

The Grad-Shafranov equation is an elliptic PDE for the poloidal magnetic flux ψ that labels the magnetic surfaces in an axisymmetric plasma equilibrium. The equation contains two *arbitrary* functions $p(\psi)$ and $F(\psi)$ that specify the dependence of the kinetic pressure and the poloidal plasma current on the magnetic flux ψ.

Accordingly, the Grad-Shafranov equation is, in general, a nonlinear PDE and its solution rely on numerical methods. However, for some choices of the arbitrary functions, the equation becomes linear and separable, and the boundary value problem can be solved by superposition of independent solutions. Various classes of analytical solutions have been introduced along the years,[5–11] usually involving linear and quadratic dependences of p and F^2 on ψ. These choices impose some inherit restrictions on the possible current density profiles, and relations between the physical parameters, but, in general, provide good magnetic topology and safety factor profiles.

In this work, we study a class of exact solutions resulting when the pressure is a linear function of ψ and the squared poloidal current is a quadratic function of ψ.[9] These solutions are characterized by an eigenvalue that is related with the equilibrium parameters of an axisymmetric plasma,

specifically, the Shafranov shift Δ, the safety factor at the magnetic axis q_{ax}, and the fraction of diamagnetic reduction of the toroidal field. This relation allows us to establish the limits of the model and its parameters, and, using physical arguments, we define a region of consistent solutions in the parameters space.

Then, we employ the analytical solutions of the Grad-Shafranov equation to build a predictive solver that allows to specify the geometrical properties of the toroidal plasma, namely, the aspect ratio ϵ, triangularity δ, elongation κ, and X-point, for a given set of physical parameters $\{\Delta, q_{ax}, f, \beta\}$.

The treatment presented in this work potentiate the use of this class of solution for predictive equilibrium calculations and to our knowledge the relations introduced here have not been presented elsewhere and provide a valuable tool for the construction of analytical equilibria. The whole treatment was done in dimensionless variables, so that the results can be properly scaled to any case of interest using a couple of machine parameters, the major radius R_0 and the toroidal vacuum field B_0.

The manuscript is organized as follows. In Sec. II, we present a short survey on hydromagnetic equilibrium with the model considered in this work and the analytical solutions to the Grad-Shafranov equation; then, in Sec. III, we study the relations between the physical parameters and the solution parameters. In Sec. IV, we introduce a numerical method to solve the boundary value problem, and in Sec. V, we give some examples of equilibrium calculations performed with this method and present our conclusions in Sec. VI.

II. ANALYTICAL SOLUTIONS

For ideal plasmas, the equilibrium between the kinetic and magnetic forces requires that

$$\vec{j} \times \vec{B} = \nabla p, \tag{1}$$

---

a)Electronic mail: dciro@if.usp.br
b)Electronic mail: ibere@if.usp.br

everywhere inside the plasma. Here, p, $\vec{j}$, and $\vec{B}$ are the kinetic plasma pressure, current density, and magnetic field, respectively. Assuming that the system is axisymmetric and using the Ampère's law, the equilibrium problem is reduced to the Grad-Shafranov equation[1–3]

$$R^2 \nabla \cdot \left(\frac{\nabla \psi}{R^2} \right) = -\mu_0 R^2 \frac{dp}{d\psi} - F \frac{dF}{d\psi} = -\mu_0 R j_\phi. \quad (2)$$

Here, R is the distance to the symmetry axis and $2\pi\psi(R,z)$ is the poloidal magnetic flux, calculated though a disk of radius R at the height z. The arbitrary function $p(\psi)$ represents the kinetic pressure at the level surface $\psi(R,z) = \text{const.}$, and $2\pi\mu_0^{-1}F(\psi)$ is the poloidal plasma current enclosed by that surface. The magnetic field lines lie on the magnetic surfaces $\psi(R,z) = \text{const.}$, which are also isobarics. Finally, the second equality in Eq. (2) relates the toroidal (azimuthal) current density with the arbitrary functions $p(\psi)$ and $F(\psi)$.

From this point, all the calculations are performed in dimensionless variables, so that the results can be scaled to any machine size and physical parameters. In dimensionless form, the Grad-Shafranov equation becomes

$$\frac{\partial^2 \bar\psi}{\partial x^2} - \frac{1}{x}\frac{\partial \bar\psi}{\partial x} + \frac{\partial^2 \bar\psi}{\partial y^2} = -\varphi^2 \left(\frac{\tilde\beta}{2} x^2 \frac{d\bar p}{d\bar\psi} + \bar F \frac{d\bar F}{d\bar\psi} \right), \quad (3)$$

where $\bar\psi(x,y) = \psi(R,z)/\psi_{ax}$ is the normalized poloidal magnetic flux, and ψ_{ax} is the flux at the magnetic axis of the plasma. The variables $(x,y) = (R/R_0, z/R_0)$ are the normalized cylindrical coordinates, with R_0 as the major radius of the plasma measured to the center of the poloidal cross section. The normalized arbitrary functions are $\bar p(\bar\psi) = p(\psi)/p_{ax}$ and $\bar F(\bar\psi) = F(\psi)/R_0 B_0$, where p_{ax} is the kinetic pressure at the magnetic axis and B_0 is the vacuum toroidal field at R_0. A characteristic beta was defined as $\tilde\beta = 2\mu_0 p_{ax}/B_0^2$ and the parameter $\varphi = R_0^2 B_0/\psi_{ax}$ characterizes the ratio of toroidal and poloidal magnetic fluxes.

In regular discharges, the toroidal current density does not invert in the plasma domain and the poloidal magnetic field always curls in the same direction about the magnetic axis. From this, the poloidal flux changes monotonically from the plasma edge to the magnetic axis. If we set $\bar\psi = 0$ at the plasma edge and require a first order dependence of the kinetic pressure on $\bar\psi$, it becomes simply

$$\bar p(\bar\psi) = \bar\psi. \quad (4)$$

This guarantees the vanishing of the pressure at the plasma edge and a maximum value at the magnetic axis. To set the form of the poloidal current $F(\psi)$, notice that the toroidal magnetic field has the form

$$\bar B_\phi = \frac{\bar F(\bar\psi)}{x}. \quad (5)$$

This field must tend to its vacuum form $B_\phi^v = 1/x$ at the plasma edge where the plasma density vanishes. Then, the poloidal current must satisfy $\bar F(0) = 1$. Requiring a second order dependence of $\bar F^2$ on $\bar\psi$ leads the general form

$$\bar F^2(\bar\psi) = a\bar\psi^2 + 2b\bar\psi + 1, \quad (6)$$

where the parameters a and b must be related to the equilibrium parameters. Using these arbitrary functions, the Grad-Shafranov (3) equation takes the linear form

$$\frac{\partial^2 \bar\psi}{\partial x^2} - \frac{1}{x}\frac{\partial \bar\psi}{\partial x} + \frac{\partial^2 \bar\psi}{\partial y^2} = -\varphi^2 \left(\frac{\tilde\beta}{2} x^2 + a\bar\psi + b \right). \quad (7)$$

The poloidal flux is a superposition of a homogeneous solution ψ_h and a particular solution ψ_p. Assuming that ψ_p depends only on even powers x, the particular solution may take the form

$$\psi_p = -\frac{\tilde\beta}{2a}x^2 - \frac{b}{a}. \quad (8)$$

Other choices lead to infinite series expansions that unnecessarily complicate the analysis or provide solutions that appear in the homogeneous solution.

To solve the homogeneous equation, define $s^2 = a\varphi^2$ for $a > 0$ and $s^2 = -a\varphi^2$ for $a < 0$, so that s is always a real number. Then, we write the homogeneous equation as an eigenvalue problem

$$\frac{\partial^2 \psi_h}{\partial x^2} - \frac{1}{x}\frac{\partial \psi_h}{\partial x} + \frac{\partial^2 \psi_h}{\partial y^2} = \mp s^2 \psi_h. \quad (9)$$

This can be solved by separation of variables with separation constants α, γ related to the eigenvalue through $\pm\alpha^2 \pm \gamma^2 = \pm s^2$.

For $a > 0$, the homogeneous solution is a linear superposition of the following functions:

$$\psi_h(x,y) = \begin{cases} x[I_1, K_1(\alpha x)][\sin, \cos(\gamma y)], & \gamma^2 = \alpha^2 + s^2 \\ [1, x^2][\sin, \cos(sy)], & \alpha = 0 \\ x[J_1, Y_1(\alpha x)][\sin, \cos(\gamma y)], & \gamma^2 = s^2 - \alpha^2 \\ x[J_1, Y_1(sx)][1, y], & \gamma = 0 \\ x[J_1, Y_1(\alpha x)][\sinh, \cosh(\gamma y)], & \gamma^2 = \alpha^2 - s^2, \end{cases} \quad (10)$$

where J_1, Y_1, K_1, I_1 are the Bessel and Bessel modified functions of first order and we have used the abbreviated notation $[f_1, f_2(x)][g_1, g_2(y)] = c_1 f_1(x) g_1(y) + c_2 f_1(x) g_2(y) + c_3 f_2(x) g_1(y) + c_4 f_2(x) g_2(y)$, with c_i as arbitrary constants. For the cases with $\alpha = 0$ or $\gamma = 0$, we use the dominant terms of the Bessel and harmonic functions for small arguments. This gives the same solutions that solving again the PDE (9) with a single separation constant.

Another possible solution can be obtained without separating variables and assuming spherical symmetry $\psi_h(x,y) = \psi_h(r)$ with $r = \sqrt{x^2 + y^2}$. In this case, the eigenvalue problem (9) becomes

$$\frac{d^2}{dr^2}\psi_h(r) = -s^2\psi_h(r), \quad (11)$$

with solutions

$$\psi_h = \sin(sr), \cos(sr). \quad (12)$$

Formally, the functions in Eq. (12) may be expanded as a continuous superposition of the functions in Eq. (10), and its involvement in the poloidal flux expansion includes a broad range of solutions. The superposition of spherical and cylindrical functions eases the production of D-shaped magnetic surfaces. So, including this type of solution has an important role in the shaping of the magnetic surfaces to describe the equilibrium in small aspect-ratio devices.

In analogy, for $a < 0$, the homogeneous solution is a superposition of

$$\psi_h(x,y) = \begin{cases} x[J_1, Y_1(\alpha x)][\sinh, \cosh(\gamma y)], & \gamma^2 = \alpha^2 + s^2 \\ [1, x^2][\sinh, \cosh(sy)], & \alpha = 0 \\ x[I_1, K_1(\alpha x)][\sinh, \cosh(\gamma y)], & \gamma^2 = s^2 - \alpha^2 \\ x[I_1, K_1(sx)][1, y], & \gamma = 0 \\ x[I_1, K_1(\alpha x)][\sin, \cos(\gamma y)], & \gamma^2 = \alpha^2 - s^2 \end{cases} \tag{13}$$

and the spherical solutions

$$\psi_h = \sinh(sr), \cosh(sr). \tag{14}$$

In Fig. 1, we arrange the solutions of Eq. (9) in the parameter space $\alpha - \gamma$; this illustrates the relation between the forms of the functions and the possible values of α, γ.

In general, to solve a boundary value problem, we will express the poloidal flux as

$$\bar{\psi}(x,y) = -\frac{b}{a} - \frac{\tilde{\beta}}{2a}x^2 + c_0 G(sr) + \sum_{\alpha,\gamma} c_{\alpha,\gamma} B(\alpha x) H(\gamma y), \tag{15}$$

where the form of the spherical solution G and the functions B and H depend on the sign of a (Fig. 1). The values of the parameters α, γ, and s must be adjusted to satisfy the boundary conditions and the number of elements in the sum is, in principle, arbitrary. The superposition can also be expressed as an integral, but from the numerical point of view we only work with discrete values of α and γ.
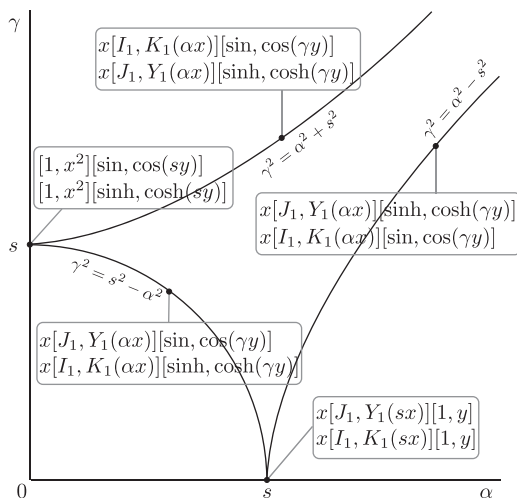

FIG. 1. Different forms of the solutions to the eigenvalue problem respect to the parameter space $\alpha - \gamma$. The upper functions on each box correspond to the solutions for $a > 0$ and the bottom for $a < 0$.

III. EQUILIBRIUM PARAMETERS

Before dealing with the numerical method to solve the boundary value problem, we need to establish relations between physical parameters and the parameters of the analytical solution (15).

From the toroidal magnetic field (5), the requirement for a diamagnetic plasma is $\bar{F}(\bar{\psi}) \lesssim 1$ on the plasma domain $0 \leq \bar{\psi} \leq 1$. To keep track of this condition, we define the constant $f = \bar{F}(1)$ and use it instead b in the poloidal flux expansion. Using Eq. (6), we obtain $2b = f^2 - 1 - a$, and the squared poloidal current becomes

$$\bar{F}^2(\bar{\psi}) = a\bar{\psi}(\bar{\psi} - 1) - (1 - f^2)\bar{\psi} + 1. \tag{16}$$

This form is more convenient to define explicitly the diamagnetic reduction of the toroidal magnetic field inside the plasma or its increase in paramagnetic cases. Using Eq. (16), the toroidal current density in units of $B_0/\mu_0 R_0$ becomes

$$\bar{j}_\phi = \frac{\varphi}{2x}\left[\tilde{\beta}x^2 + a(2\bar{\psi} - 1) + f^2 - 1\right]. \tag{17}$$

At the magnetic axis, the safety factor can be written[12]

$$q_{ax} = \frac{\bar{B}_\phi}{|\partial_x(x\bar{B}_y)\partial_y(x\bar{B}_x)|^{1/2}}, \tag{18}$$

where $\{\bar{B}_x, \bar{B}_\phi, \bar{B}_y\}$ are the cylindrical components of the magnetic field in units of B_0, and $\{\partial_x, \partial_y\}$ is a compact notation for the partial derivatives. In general, close to the magnetic axis, the magnetic surfaces have an elliptical cross section with major and minor semi-axes $\Delta y, \Delta x$. It can be shown that, in the limit $\Delta x, \Delta y \to 0$, the ratio of these lengths satisfy

$$\lim_{\Delta y, \Delta x \to 0}\left(\frac{\Delta y}{\Delta x}\right)^2 = \kappa_{ax}^2 = -\frac{\partial_x(x\bar{B}_y)}{\partial_y(x\bar{B}_x)}, \tag{19}$$

where the partial derivatives are evaluated on the magnetic axis. Equation (19) is the squared elongation of the innermost magnetic surfaces κ_{ax}. Using this and the Ampère's law

$$\bar{j}_\phi = \partial_y\bar{B}_x - \partial_x\bar{B}_y, \tag{20}$$

the safety factor on the magnetic axis becomes

$$q_{ax} = \frac{2\bar{B}_\phi}{(1 + \Delta)\bar{j}_{ax}}\left(1 + \frac{1}{2}\frac{\lambda^2}{1 + \lambda}\right), \tag{21}$$

with $\bar{j}_{ax}$ as the toroidal current density on the magnetic axis, Δ as the Shafranov shift in units of R_0 and, $\lambda = \kappa_{ax} - 1$, characterizes the ellipticity of the surfaces close to the magnetic axis. For circular surfaces, $\lambda = 0$, leading to the circular section low-beta limit.[12] The elongation of the magnetic surfaces provides a second order correction to the safety factor. Setting $\bar{\psi} = 1$ and $x = 1 + \Delta$ in Eq. (17) to replace $\bar{j}_{ax}$ in Eq. (21), and replacing Eq. (16) in Eq. (5), we obtain

$$q_{ax} = \frac{4f\left[1 + 0.5\lambda^2/(1 + \lambda)\right]}{\varphi(1 + \Delta)\left[\tilde{\beta}(1 + \Delta)^2 + a + f^2 - 1\right]}. \tag{22}$$

Now, this relation is used to write φ in terms of the other parameters, and is replaced in the eigenvalue equation

$$s = \sqrt{|a|}\varphi. \tag{23}$$

This gives s in terms of $q_{ax}, \lambda, \Delta, f$ and the adjustable parameter a

$$s = \frac{4f\sqrt{|a|}}{\tilde{q}_{ax}(1+\Delta)\left[\tilde{\beta}(1+\Delta)^2 + a + f^2 - 1\right]}, \tag{24}$$

with $\tilde{q}_{ax} = q_{ax}/[1 + 0.5\lambda^2/(1+\lambda)]$. For a predictive calculation, the value of q_{ax} can be settled and the internal elongation κ_{ax} can be estimated from the plasma edge elongation. The parameters f, Δ, and $\tilde{\beta}$ can also be pre-established. For instance, in a usual diamagnetic configuration $f \lesssim 1$, $q_{ax} \gtrsim 1$, and $\Delta \approx 10^{-1}$. To estimate the characteristic beta $\tilde{\beta}$, we use Eq. (4), and the definition of the toroidal beta $\beta_t = 2\mu_0\langle p\rangle/B_0^2$, leading to

$$\beta_t = \tilde{\beta}\langle\bar{\psi}\rangle, \tag{25}$$

where $\langle\rangle$ denotes a volume average in the plasma domain. In a high-beta plasma, the toroidal beta dominates the value of the total beta, $\beta \approx \beta_t$.[13] Also, since $\bar{\psi} = 0$ at the plasma edge and $\bar{\psi} = 1$ on the magnetic axis, we can expect $\langle\bar{\psi}\rangle \approx 0.5$. Then, for a given value of beta, we can approximate the characteristic beta by

$$\tilde{\beta} \approx 2\beta. \tag{26}$$

To set the eigenvalue of the problem we need to know a in Eq. (24). We can define a as an adjustable parameter, but its range of allowed values must be established in a physical basis. To do this, we require the toroidal current density not to change its sign because it is mainly created by an inductive electric field. The signs of j_ϕ and ψ_0 must be the same, consequently the signs of $\bar{j}_\phi$ and φ in Eq. (17) are the same, leading to the condition

$$\tilde{\beta}x^2 + a(2\bar{\psi} - 1) + f^2 - 1 \geq 0, \tag{27}$$

in the whole plasma domain. Evaluating Eq. (27) in the magnetic axis and on the innermost boundary point leads to

$$1 - f^2 - \tilde{\beta}(1+\Delta)^2 \leq a \leq \tilde{\beta}(1-\epsilon)^2 + f^2 - 1, \tag{28}$$

where ϵ is the aspect ratio of the plasma. Now, the condition for no poloidal current density inversions, comes from requiring the poloidal current $\bar{F}(\bar{\psi})$ to be a monotonic decreasing function of $\bar{\psi}$, i.e., $\bar{F}' < 0$. Using Eq. (16), we obtain the condition

$$f^2 - 1 < a < 1 - f^2. \tag{29}$$

This condition is useful to identify the parameters for poloidal current density inversions that may be required to describe the reversed magnetic shear equilibria emerging in situations with large bootstrap fractions. Following the conditions (29) and (28), we can identify the regions of interest in the parameter space $a - \tilde{\beta}$ (Fig. 2).
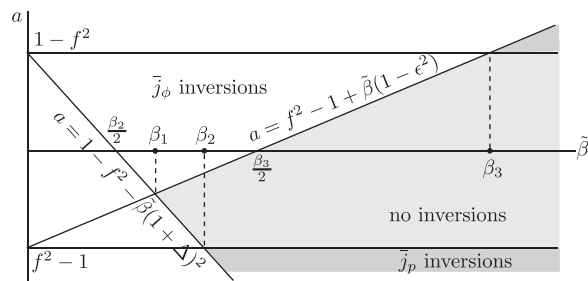

FIG. 2. The light region correspond to pairs $(a, \tilde{\beta})$ for which there are no toroidal or poloidal current density inversions. In the dark region the poloidal current density inverts but the toroidal do not.

In Fig. 2, we depict the regions for poloidal current inversion $\bar{j}_p$, and no-inversions using the definitions

$$\beta_2 = 2\frac{1-f^2}{(1+\Delta)^2}, \quad \beta_3 = 2\frac{1-f^2}{(1-\epsilon)^2} \tag{30}$$

and $1/\beta_1 = 1/\beta_2 + 1/\beta_3$. The restrictions over the allowed values of a and $\tilde{\beta}$ defines through Eq. (24) the set of allowed eigenvalues s that gives physical solutions to the boundary value problem. Given the form of the solutions in Eq. (15), it is more convenient to adjust the eigenvalue s than the parameter a. For this, we invert Eq. (24) to write a in terms of s and the physical parameters $\tilde{q}_{ax}, \eta, \Delta, f, \tilde{\beta}$

$$a_\pm(s) = 1 - f^2 - \tilde{\beta}(1+\Delta)^2 \pm \frac{8f^2}{\tilde{q}_{ax}^2 s^2(1+\Delta)^2}$$
$$\times \left(1 - \sqrt{1 \pm \frac{\tilde{q}_{ax}^2 s^2(1+\Delta)^2}{4f^2}\left[1 - f^2 - \tilde{\beta}(1+\Delta)^2\right]}\right), \tag{31}$$

where $a_+(s)$ is valid for $a > 0$ and $a_-(s)$ for $a < 0$.

In Fig. 3, we depict the regions of interest in the parameter space $s - \tilde{\beta}$ using the definition

$$A = \frac{2}{\tilde{q}_{ax}(1+\Delta)}\frac{f}{\sqrt{1-f^2}}. \tag{32}$$

As in Fig. 2, the region with $a < 0$ is larger that the corresponding to $a > 0$. Also, large values of s lead to poloidal current inversions, except for a narrow region of $\tilde{\beta}$ between β_1 and β_2.
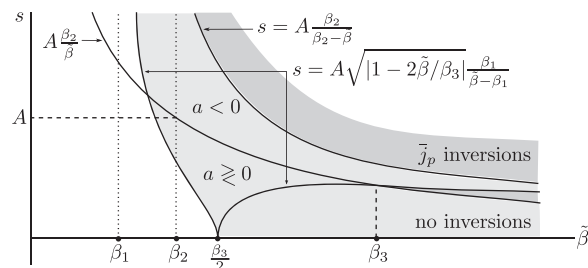

FIG. 3. Like in Fig. 2, the light region correspond to pairs $(s, \tilde{\beta})$ for which there are no current density inversions and the darker region lead to poloidal current density inversions. As negative values of s are not allowed the regions for $a < 0$ and $a > 0$ share a portion of the parameter space.

IV. NUMERICAL METHOD

Now that we have characterized the equilibrium solutions respect to their position in the parameters space, we can develop a systematic method to build analytical solutions with some desired equilibrium properties.

Using $2b = f^2 - 1 - a$ and Eq. (31), the poloidal magnetic flux (15) can be casted like

$$\bar{\psi}(x,y) = \frac{1}{2} + \frac{1 - f^2 - \tilde{\beta}x^2}{2a_\pm(s)} + c_0 G(sr) + \sum_i c_i B(\alpha_i x) H(\gamma_i y),$$
(33)

with $\gamma_i = \gamma(\alpha_i, s)$ (see Fig. 1). The sign of a determines its form in Eq. (33) and the functions G, B, and H as explained in Sec. II. The sign of a is then kept unchanged during any optimization procedure that modifies the eigenvalue s, the coefficients c_i, and the parameters α_i.

The Levenberg–Marquardt algorithm[14] is used to adjust the linear and nonlinear parameters involved in this problem. This method gives good convergence for reasonable choices of the starting parameters. In general, the iterative process consists in the minimization of the error functional

$$\varepsilon(\vec{k}) = \sum_{i=1}^{N} [\psi_i - \bar{\psi}(p_i, \vec{k})]^2,$$
(34)

where $p_i = (x_i, y_i)$ are points where we know the numerical values of the poloidal flux ψ_i, and $\bar{\psi}(p_i, \vec{k})$ is our approximation to that value through Eq. (33) for a given set of M parameters $\vec{k} = \{s, \{c_i\}, \{\alpha_i\}\}$. The minimization of Eq. (34) is done by successive variations of $\vec{k}$

$$\vec{k}_1 = \vec{k}_0 + \vec{\delta},$$
(35)

where $\vec{\delta}$ must satisfy $\varepsilon(\vec{k} + \vec{\delta}) < \varepsilon(\vec{k})$ and is obtained by solving the linear problem

$$(J^T J - \lambda I)\vec{\delta}(\lambda) = J^T[\vec{y} - \vec{f}(\vec{k})].$$
(36)

Here, I is the $M \times M$ identity matrix, λ is an adjustable parameter and the vectors are defined by

$$\vec{y} = (\psi_1, \psi_2, ..., \psi_N)^T,$$
(37)

$$\vec{f}(\vec{k}) = (\bar{\psi}(p_1, \vec{k}), \quad \bar{\psi}(p_2, \vec{k}), ..., \bar{\psi}(p_N, \vec{k}))^T.$$
(38)

J is an $M \times N$ matrix with entries

$$J_{i,j} = \frac{\partial \bar{\psi}(p_j, \vec{k})}{\partial k_i},$$
(39)

that in this case can be calculated analytically. To update $\vec{k}$ and λ, we calculate the errors for $\vec{\delta}(\lambda)$ and $\vec{\delta}(\lambda')$ where $\lambda' = r\lambda$ and $0 < r < 1$. Then $\vec{k}$ and λ are updated with the variation that gives the largest error reduction. If neither reduces the error we do $\lambda \to \lambda/r$ and repeat the previous step. Following this procedure, we guarantee a rapid convergence far from the minimum and more refined steps close to it.

The points where the poloidal flux is known are on the plasma edge, where $\psi_i = 0$ and the magnetic axis where $\psi_N = 1$. To describe the plasma edge, we can use a parametric equation containing the relevant geometry

$$x_b(\theta) = 1 + \epsilon \cos(\theta + \alpha \sin \theta),$$
(40)

$$y_b(\theta) = \epsilon \kappa \sin \theta,$$
(41)

$$\delta = \sin \alpha.$$
(42)

This describes a D-shape with triangularity δ, elongation κ, and minor radius ϵ. In the case of a single or double null configuration, we can trace straight lines that meet at the X-point at a distance $\eta\epsilon$ from the center with a desired angle ξ (see Fig. 4). For given values of ξ and η, the positions of the X-point p_3, and the tangency points p_1 and p_2 are uniquely determined and can be found by solving numerically an implicit equation.

V. RESULTS AND DISCUSSION

In the following, the numerical optimization described in Sec. IV will be used to find possible equilibrium configurations with realistic features in cases with normal and reversed magnetic shear.

A. Normal shear equilibrium

As a first example, the optimization algorithm is used to describe a shaped plasma with the parameters in Table 1. As we cannot preset the value of β in our method, we will set the value of $\tilde{\beta}$ following Eq. (26), assuming $\langle \bar{\psi} \rangle \approx 0.5$ for a
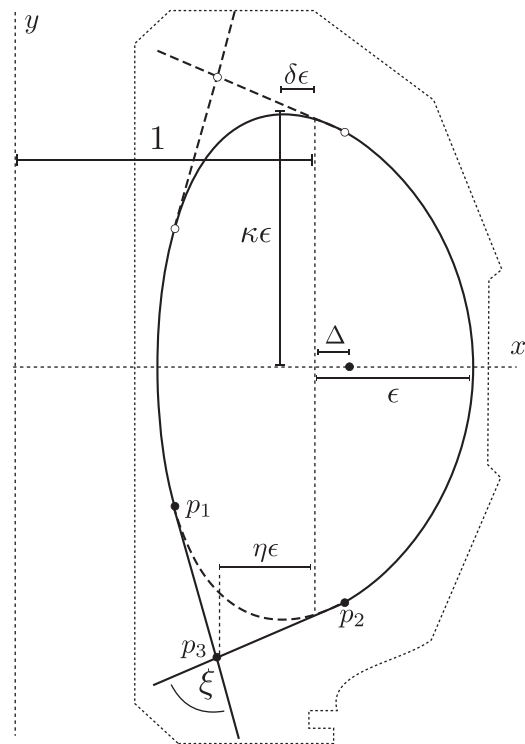

FIG. 4. The plasma edge is modeled by merging a D-shape with two tangent straight lines starting at p_1, p_2 and crossing at the X-point p_3. The center of the column is at $x = 1$ and the magnetic axis is displaced by Δ.

TABLE I. Desired parameters.

ϵ	κ	δ	ξ	η	Δ	q_{ax}	β
0.5	1.5	0.1	0.4π	0.6	0.1	1.2	10%

usual discharge. From this we can estimate $\tilde{\beta} \approx 0.2$ as a starting guess for the optimization. Also, we cannot preset the internal elongation of the magnetic surfaces, so we approximate $\kappa_{ax} \sim \kappa$ and calculate the value of $\tilde{q}_{ax}$ to feed the function $a(s)$ in Eq. (31). After the equilibrium is found, we can measure the internal elongation to find the real preset value of q_{ax}. We also start assuming a toroidal field reduction of 5% relative to the vacuum value, i.e., $f \approx 0.95$. There is a close relation between the toroidal field fraction f and the value of $\tilde{\beta}$, so we perform several runs for different combinations of $\tilde{\beta}$ and f until we find the combination $(\tilde{\beta}, f) = (0.26, 0.97)$, leading to the best error reduction and magnetic topology for the chosen expansion of the flux $\bar{\psi}$.

To choose the basis we first set $a > 0$ that corresponds to the solution (10) and leads to a maximum of the toroidal current density inside the plasma (see Eq. (17)), otherwise we could get a minimum which is only relevant in cases with reversed magnetic shear. The choice of the basis elements to expand the poloidal flux is somewhat intuitive. We start by choosing the functions on each branch of Fig. 1, then we turn on/off the different elements of the basis to see if the performance of the method is improved. After a few trials, we keep the expansion that best minimizes the error, presenting the most physically relevant plasma profiles and topology of the magnetic surfaces. The resulting expansion is

$$\bar{\psi}(x,y) = 1/2 + (1 - f^2 - \tilde{\beta}x^2)/2a(s) + (c_1 + c_2 y)xY_1(sx)$$
$$+ c_3 \sin(sy) + c_4 \cos(sy) + c_5 \sin(sr) + c_6 \cos(sr)$$
$$+ c_7 x J_1(\alpha_7 x)\sin(\gamma_7 y) + c_8 x J_1(\alpha_8 x)\cos(\gamma_8 y)$$
$$+ c_9 x Y_1(\alpha_9 x)\sin(\gamma_9 y) + c_{10} x Y_1(\alpha_{10} x)\cos(\gamma_{10} y)$$
$$+ c_{11} x K_1(\alpha_{11} x)\sin(\gamma_{11} y) + c_{12} x K_1(\alpha_{12} x)\cos(\gamma_{12} y)$$
$$+ c_{13} x J_1(\alpha_{13} x)\cos(\gamma_{13} y) + c_{14} x Y_1(\alpha_{14} x)\cos(\gamma_{14} y),$$
$$(43)$$

with $r = \sqrt{x^2 + y^2}$. Using the restrictions (28) and (29) over a, we were able to estimate the starting eigenvalue on $s \approx 3.0$, and the initial values of the starting parameters were chosen to be $\alpha_{7-10} = 0.5s$, $\alpha_{11,12} = 3.5s$, and $\alpha_{13,14} = 0.3s$. These values evolve independently of s during the optimization process, then, they will spread in the parameter space $\alpha - \gamma$. The initial values of the expansion coefficients $\{c_i\}$ are calculated by solving the linear problem of minimizing the error $\varepsilon(\{c_i\})$ for s, $\{\alpha_i\}$ fixed on the starting values.

In Fig. 5, we can see the evolution of the solution parameters as the error is reduced from 26.7 to 2.4×10^{-3} in 200 iterations of the method, when the parameters and the error do not change significantly the run ends.

After the minimum is reached and we are satisfied with the plasma shape, we can calculate the relevant plasma profiles. In Fig. 6(left), we depict the resulting topology of the magnetic surfaces and the 50 control points used in the
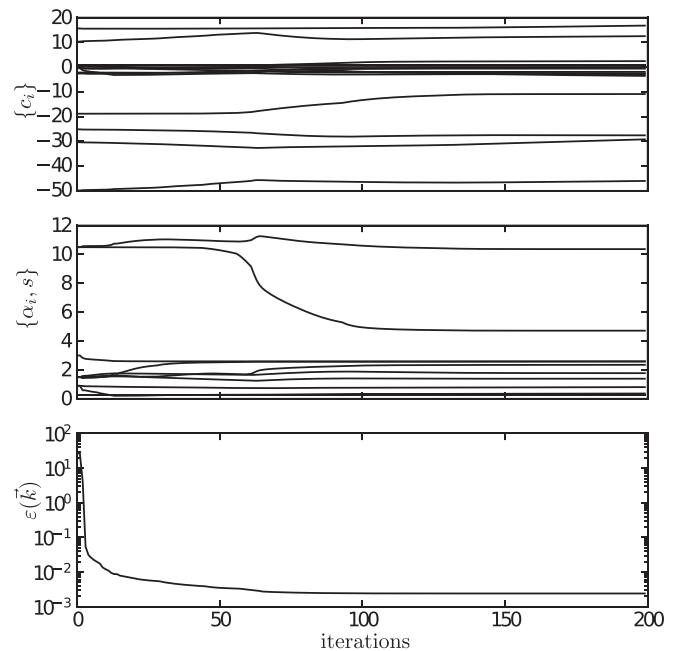

FIG. 5. Traces of the expansion coefficients $\{c_i\}$ and the nonlinear parameters s, $\{\alpha_i\}$ for 200 iterations of the minimization method. The eigenvalue s stabilizes at 2.69 and the error at 2.4×10^{-3}.

method, $\psi_{1-49} = 0$ for the plasma edge and $\psi_{50} = 1$ at the magnetic axis. The plasma edge is in good agreement with the desired shape and the magnetic surfaces behave as expected with the magnetic axis slightly displaced from the desired position.

We use Eqs. (5), (16), and (31) to calculate $\bar{B}_\phi$ and compare with the vacuum toroidal field $\bar{B}_\phi^v = 1/x$. In Fig. 6 (right), we can see the reduction of the toroidal field due to the diamagnetic effect controlled by f. The pressure profile is by definition the same of $\bar{\psi}$ and the toroidal current density $\bar{j}_\phi$ is calculated with Eq. (17) using the relations (23), (24), and (31).

For $\tilde{\beta} = 0.26$, the obtained eigenvalue is slightly outside the shaded region in Fig. 3, accordingly, there is a moderated
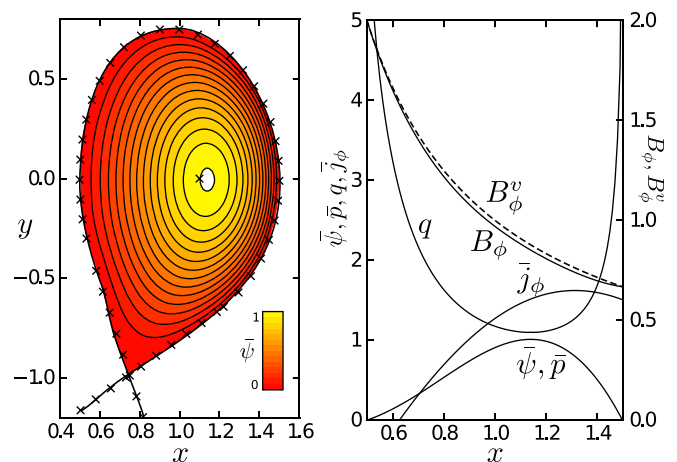

FIG. 6. In the left, the poloidal magnetic flux contours show good agreement with the imposed control points (×), at the edge and magnetic axis. In the right, the resulting profiles of $q(x), B_\phi(x), \bar{\psi}(x), \bar{p}(x)$ for a transversal cut $y = 0$, behave as expected for a divertor discharge, and the vacuum magnetic field $\bar{B}_\phi^v = 1/x$ stands above B_ϕ, illustrating the diamagnetic effect of the poloidal plasma current.

inversion in j_ϕ coming from the inherit restrictions of the model, and, in addition, $\bar{j}_\phi$ does not vanish at the edge in the low field side.

To understand the $\bar{j}_\phi$ profile, notice in Eq. (17), that the toroidal current density is not constant at the plasma edge, where $\bar{\psi} = 0$, but changes with the radial distance x. Consequently, the current density cannot vanish in the low and high field side simultaneously. This is a direct consequence of the choice of the profiles of $p(\psi)$ and $F(\psi)$ that makes linear the Grad-Shafranov equation (3), and such unphysical behavior is acceptable when working with analytical models.

The safety factor $q(\bar{\psi})$ is the constant ratio $d\phi/d\vartheta$ of the toroidal and poloidal angles subtended by the magnetic line as it wanders over its invariant surface. The poloidal angle ϑ is not uniform in the Cartesian space $\{x, y\}$, but the toroidal one is, so, we can calculate $q(\bar{\psi})$ by following the magnetic line until it completes a full poloidal cycle, then we use

$$q(\bar{\psi}) = \frac{\Delta\phi}{2\pi}. \tag{44}$$

Doing this for a set of initial conditions in the line $y = 0$, we get the q-profile in Fig. 6(right). The internal elongation of the flux surfaces was calculated as $\kappa_{ax} = 1.57$, so $\lambda = 0.57$; the value $\tilde{q}_{ax} = 1.1$ was used in the calculations, so the actual preset value of q_{ax} was $\tilde{q}_{ax}[1 + 0.5\lambda^2/(1 + \lambda)] = 1.22$, which is very close to that appearing in Table 1. The profile value $q_{min} = 1.096$ is close to this value, and the safety factor at the 95% flux surface (in our case $\bar{\psi} = 0.05$), is $q_{95} = 4.515$. This is a typical value for a divertor discharge and was not preset in the analytical solution, but comes naturally from the elements of the expansion and the boundary conditions. The volume averaged poloidal flux is $\langle\psi\rangle = 0.45$, then, from Eq. (25) the toroidal beta is $\beta_t = 11.7\%$. We also calculate the poloidal beta given by $\beta_p = 2\mu_0\langle p\rangle/\bar{B}_p^2$ where $\bar{B}_p = \mu_0 I_0/2\pi a\kappa$, a is the minor radius, κ is the elongation, and I_0 is the plasma current. In dimensionless variables, we can write this like

$$\beta_p = \tilde{\beta}(2\pi\epsilon\kappa)^2 \frac{\langle\bar{\psi}\rangle}{\bar{I}_0^2}, \tag{45}$$

where $\bar{I}_0 = \int\int \bar{j}_\phi(x, y)dxdy$ is the plasma current in units of $R_0 B_0/\mu_0$, namely, the current used to create the vacuum toroidal field. Replacing our values, we obtain $\beta_p = 2.86$, then we can calculate the total beta using $\beta^{-1} = \beta_t^{-1} + \beta_p^{-1}$, and we obtain $\beta = 11.2\%$ that is just 1.2% above the desired value.

Table 2 summarizes the results presented for this equilibrium. For the chosen poloidal flux expansion (43), the optimization method led to good agreement with the expected values of Table 1, and reasonable prediction for the

values of the plasma current $\bar{I}_p$, the poloidal beta β_p, total beta β, and the 95% flux surface safety factor.

B. Reversed shear equilibrium

In plasmas with high bootstrap fraction, the current density profile is fundamentally changed, presenting a central minimum and maximum off-axis. This behavior leads to a non-monotonic safety factor profile with maximum at the magnetic axis and minimum off-axis. In divertor discharges, the minimum in q is reinforced by the growth of q to the plasma edge, where it diverges. For this case, we choose a double null equilibrium with the parameters in Table 3. In analogy to the previous case, using $\kappa_{ax} \sim \kappa$, the value $\tilde{q}_{ax} = 3.46$ was estimated. We start with the guess $\tilde{\beta} = 0.14$ and $f = 0.95$ and perform several runs changing these values for a given choice of the poloidal flux expansion. The central reversed magnetic shear was obtained for $f \gtrsim 1$, making the plasma slightly paramagnetic. Values below *one* led to non-monotonic safety factor profiles with several critical points. The parameters that best minimized the error functional were $(\tilde{\beta}, f) = (0.14, 1.05)$.

The hollow current profile requires $a < 0$, corresponding to the solution (13) of the Grad-Shafranov equation. Proceeding analogously to the previous case and using only even functions of y, we consider the following poloidal flux expansion:

$$\begin{aligned}
\bar{\psi}(x,y) = &\ 1/2 + (1 - f^2 - \tilde{\beta}x^2)/2a(s) + c_1\cosh(sr) \\
&+ (c_2 + c_3x^2)\cosh(sy) + c_4xI_1(sx) + c_5xK_1(sx) \\
&+ c_6I_1x(\alpha_6x)\cos(\gamma_6y) + c_7xK_1(\alpha_7x)\cos(\gamma_7y) \\
&+ c_8xJ_1(\alpha_8x)\cosh(\gamma_8y) + c_9xY_1(\alpha_9x)\cosh(\gamma_9y) \\
&+ c_{10}xI_1(\alpha_{10}x)\cosh(\gamma_{10}y) + c_{11}xK_1(\alpha_{11}x)\cosh(\gamma_{11}y) \\
&+ c_{12}xJ_1(\alpha_{12}x)\cosh(\gamma_{12}y) + c_{13}xY_1(\alpha_{13}x)\cosh(\gamma_{13}y),
\end{aligned} \tag{46}$$

the staring eigenvalue was established about $s \approx 8.0$, and the parameters were $\alpha_{6,7} = 1.2s$, $\alpha_{8,9} = 2.1s$, $\alpha_{10,11} = 0.6s$, and $\alpha_{12,13} = 0.8$. In this case, the optimization method performed 300 cycles and the error stabilized at 7.6×10^{-3}. The eigenvalue stabilized close to the starting value at $s = 8.492$. The resulting profiles are presented in Fig. 7.

For this equilibrium (Fig. 7), the poloidal flux and kinetic pressure present a stronger drop at the plasma edge and the toroidal magnetic field is slightly increased (5%) respect to its vacuum value, indicating a paramagnetic behavior. The obtained current density presents a large hole at the plasma center and by inherit model restrictions it can neither develop the off-axis maxima nor decrease to the plasma edge.

In this case, the actual internal elongation is $\kappa_{ax} = 1.931$, and it was used $\tilde{q}_{ax} = 3.46$ so, the actual preset safety factor

TABLE II. Obtained parameters.

Δ	$\tilde{\beta}$	f	q_{min}	q_{95}	β_t	β_p	β	$\bar{I}_0$
0.14	0.26	0.97	1.096	4.515	11.7%	2.86	11.2%	1.048

TABLE III. Desired parameters.

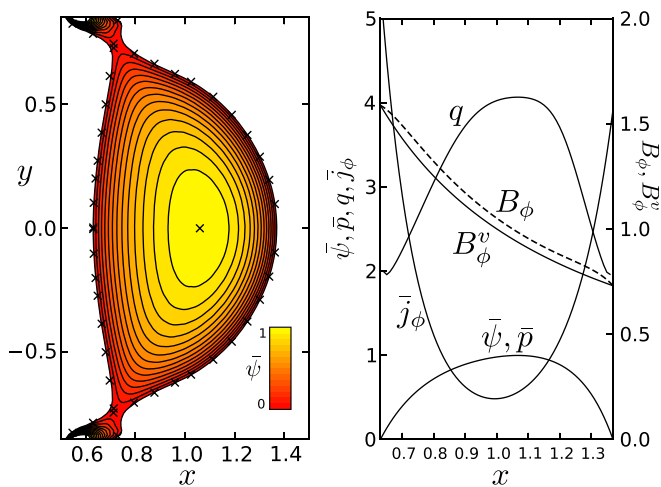| ϵ	κ	δ	ξ	η	Δ	q_{ax}	β
0.37	1.9	0.3	0.4π	0.77	0.06	4.2	7%

FIG. 7. In the left, the poloidal magnetic flux contours for a double null configuration and the control points ($\times$), at the edge and magnetic axis. In the right, the resulting profiles of $q(x), B_\phi(x), \bar\psi(x), \bar p(x)$ for a transversal cut $y = 0$, in this case we have a hollow current profile and reversed magnetic shear. The vacuum magnetic field $\bar B^v_\phi = 1/x$ stands below B_ϕ, revealing a paramagnetic behavior of the plasma.

was $q_{ax} = 4.24$, which is compatible with the numerical maximum at the magnetic axis $q_{max} = 4.06$. The q-profile also presents an off-axis minimum near the plasma edge $q_{min} = 1.96$, the minimum value, though consistent in magnitude with equilibrium reconstructions of reversed magnetic shear discharges,[15] develops very close to the 95% surface, causing an abrupt growth in q close to the separatrix. This is a consequence of the inability of the current density to decrease to the edge. Accordingly, this model is only able to represent a global reversed magnetic shear and should only be used locally to describe the central region of the plasma.

The magnetic axis is displaced by 0.6% from the desired position and the toroidal and poloidal beta are $\beta_t = 8.43\%$, $\beta_p = 0.53$, leading to $\beta = 7.27\%$ that is 0.27% above the desired value. The plasma current in units of $R_0 B_0/\mu_0$ is $\bar I_0 = 1.577$. This is a large value, e.g., if $R_0 = 1.6m$ and $B_0 = 2T$, then $I_p \approx 4MA$, which is caused by the unavoidable growth of the current density to the plasma edge.

For this equilibrium, the values of $q_{max}, q_{min}, \beta_t, \beta_p$, and β are consistent with realistic situations (see Table IV), but the model is only able to reproduce the internal plasma behavior, and more flexible profiles for q and j_ϕ requires higher powers of $\bar\psi$ on the source functions $\bar p(\bar\psi)$ and $\bar F(\bar\psi)$, and consequently, the solution of the full non-linear Grad-Shafranov equation.

VI. CONCLUSIONS

In this work, we have identified the relevant parameters of a linear model of the Grad-Shafranov equation and related them with the plasma parameters of the hydromagnetic equilibrium, revealing the consistency regions in the parameter

TABLE IV. Obtained parameters.

Δ	$\tilde\beta$	f	q_{max}	q_{min}	β_t	β_p	β	$\bar I_0$
0.067	0.14	1.05	4.06	1.96	8.43%	0.53	7.27%	1.577

space. For predictive calculations, the model parameters can be fixed and the poloidal magnetic flux becomes a linear superposition of the solutions to the linear Grad-Shafranov equation. This introduces a number of free parameters that can be adjusted numerically.

We have applied an optimization method to adjust the free parameters in a situation where the plasma edge and magnetic axis were established. This method is able to produce single or double-null equilibrium configurations with realistic geometry and parameters. It achieves good magnetic topology, safety factor profiles, realistic values of β, and allows the explicit control the amount of diamagnetism or even paramagnetism in the plasma. However, it has some inherit limitations in the current density profile due to the choice of the arbitrary functions.

The presented description of the plasma can be used globally to study the equilibrium in usual and high-β discharges and locally to describe the internal plasma in a reversed magnetic shear configuration. In both cases, the convergence to the solution is good for reasonable choices of the basis functions in the poloidal flux expansion.

[1]V. Hain, R. Lüst, and A. Schlüter, Z. Naturforschg. **12a**, 833 (1957).
[2]H. Grad and H. Rubin, in Proceedings of 2nd UN Conference on the Peaceful Uses of Atomic Energy (1958), Vol. 31, p. 190.
[3]V. Shafranov, Sov. Phys. JETP **6**, 545 (1958).
[4]V. Shafranov and L. Zakharov, Nucl. Fusion **12**, 599 (1972).
[5]L. Solov'ev, Sov. Phys. JETP **26**, 400 (1968).
[6]E. K. Maschke, Plasma Phys. **15**, 535 (1973).
[7]S. Zheng, A. Wootton, and E. Solano, Phys. Plasmas **3**, 1176 (1996).
[8]G. Ludwig, Plasma Phys. Controlled Fusion **39**, 2021 (1997).
[9]P. McCarthy, Phys. Plasmas **6**, 3554 (1999).
[10]L. Guazzotto and J. Freidberg, Phys. Plasmas **14**, 112508 (2007).
[11]A. J. Cerfon and J. P. Freidberg, Phys. Plasmas **17**, 032502 (2010).
[12]G. Bateman, *MHD Instabilities* (MIT Press, 1987), p. 220.
[13]J. Freidberg, *Ideal Magnetohydrodynamics* (Plenum Press, NY, 1987), p. 71.
[14]D. Marquardt, J. Soc. Ind. Appl. Math. **11**, 431 (1963).
[15]E. Strait, L. Lao, M. Mauel, B. Rice, T. Taylor, K. Burrell, M. Chu, E. Lazarus, T. Osborne, S. Thompson, and A. Turnbull, Phys. Rev. Lett. **75**, 4421 (1995).